

STATIC AND DYNAMIC LATERAL LOAD TESTS IN LIQUEFIED SAND FOR THE COOPER RIVER BRIDGE, CHARLESTON, SOUTH CAROLINA

Kyle Rollins¹, Seth Bowles², Luke Hales³ and Scott Ashford⁴

ABSTRACT

Lateral static and dynamic load tests were performed on two 8.5 ft diameter drilled shaft foundations at the Cooper River Bridge site in Charleston, South Carolina after liquefying the soil to a depth of 42 ft using controlled blasting. Following blasting about six times more movement was required to develop the same lateral resistance as before blasting. The maximum bending moment doubled and developed at the base of the liquefied sand. Using the moment vs. depth profiles, p-y curves for the liquefied sand were back-calculated and compared favorably with those computed with equations developed from the Treasure Island liquefaction test using a diameter correction factor of about 9. Good agreement was obtained between the measured static load-deflection curve and that computed with LPILE using the back-calculated p-y curves. Although liquefied, the sand still provided lateral resistance that was significant. Based on the dynamic testing the damping ratio for the shaft in liquefied sand was found to be between 30 and 35%. The static lateral resistance was interpreted from the dynamic test using a lumped mass approach and was found to be very similar to that measured in the static tests. The blast liquefaction technique in combination with the dynamic lateral load procedure provides a viable means for evaluating the dynamic lateral resistance of deep foundations in liquefied sand under full-scale conditions for important structures.

¹ Prof., Civil & Env. Engrg Dept., Brigham Young Univ., Provo, UT, Email: rollinsk@byu.edu

² Staff Engineer, Wright Engineers, Irvine, CA, Email: seth.bowles@gmail.com

³ ExxonMobil – Qatar, PO Box 4490, Houston, Texas 77210, Email: LHales@qatargas.com.qa

⁴ Head, School of Civil & Construction Engrg. Oregon State Univ., Corvallis, OR, USA Email: scott.ashford@oregonstate.edu

INTRODUCTION

The lateral resistance of deep foundations in liquefiable sand has been an important issue in geotechnical earthquake engineering for many years. Approaches to evaluate lateral pile resistance in liquefiable sand have included centrifuge tests (Wilson et al., 2000), large scale shaking table tests (Suzuki and Tokimatsu, 2003) and full-scale field tests using blast induced liquefaction (Rollins et al. 2005a, Weaver et al. 2005). Centrifuge testing avoids the higher cost of full-scale or large scale testing and allows an examination of multiple factors involved. Nevertheless, full-scale field testing can be particularly helpful for site-specific investigations for important bridges in seismically active areas. This was particularly true for the Arthur Ravenel Bridge which now spans the Cooper River in Charleston, South Carolina. Completed in July 2005, the Ravenel Bridge has a clear span of 1546 feet, making it the longest cable-stayed bridge in North and South America. Geotechnical investigations for the Ravenel Bridge determined that liquefaction could occur to a depth of 13 m on the eastern approach to the bridge in a repeat of the 1886 Charleston earthquake (estimated M7.3). Based on the success of the Treasure Island Liquefaction Test (TILT) in San Francisco (Ashford et al 2004, Rollins et al 2005a, Weaver et al 2005), designers included full-scale blast liquefaction testing as part of the foundation testing program for the new bridge (Camp et al 2002). Following blast-induced liquefaction, lateral load tests were performed using both conventional hydraulic load actuators and a static loading device to evaluate lateral resistance of the large diameter drilled shaft foundations anticipated for the bridge. This paper will provide a summary of the static and static load test results. Comparison of predicted and measured response will also be made using equations for the lateral resistance of deep foundations developed in the TILT project (Rollins et al 2005a).

GEOTECHNICAL SITE CHARACTERISTICS

The soil profile at the test site generally consists of alluvial sands underlain by the Ashley formation of the Cooper Group at a depth of 42 to 46 ft (13 to 14 m). This formation is known locally as the Cooper Marl. Groundwater was generally located between the ground surface and a depth about of 5 ft, depending on tidal fluctuations. The sandy sediments of the coastal plain in South Carolina are typically loose Pleistocene age materials while the Cooper Marl is an Eocene to Oligocene age marine deposit. Prior to design of the bridge, a comprehensive geotechnical investigation was carried out to define the characteristics of the subsurface materials at the site. Preliminary studies were initially performed by Parson-Brinkerhoff and more detailed investigations were subsequently performed by S&ME, Inc. Based on the test hole logs, Camp et al (2002) developed an idealized soil profile for the site with six layers. This profile, with some minor modifications, is shown in Figure 1.

The first layer typically extends from the ground surface to a depth of 5 ft (1.5 m) and consists of loose, poorly graded fine sand (SP) to silty sand (SM). In some cases, sandy clay layers were interbedded in this material. The surface sand was typically underlain by a sandy clay layer 3 to 5 ft (1.0 to 1.5 m) thick which classified as CH material. This clay layer was very soft and had an average natural moisture content of about 106%, which is approximately the same as the liquid limit suggesting that the clay is normally consolidated. The PI was typically about 70%. The third layer was also a loose, fine sand (SP) to silty sand (SM) similar to the first layer and typically extended to a depth of 18 ft (5.5 m). The fines content varied considerably with depth and from hole to hole with a range from 0.5 to 28%. The fourth layer was typically located

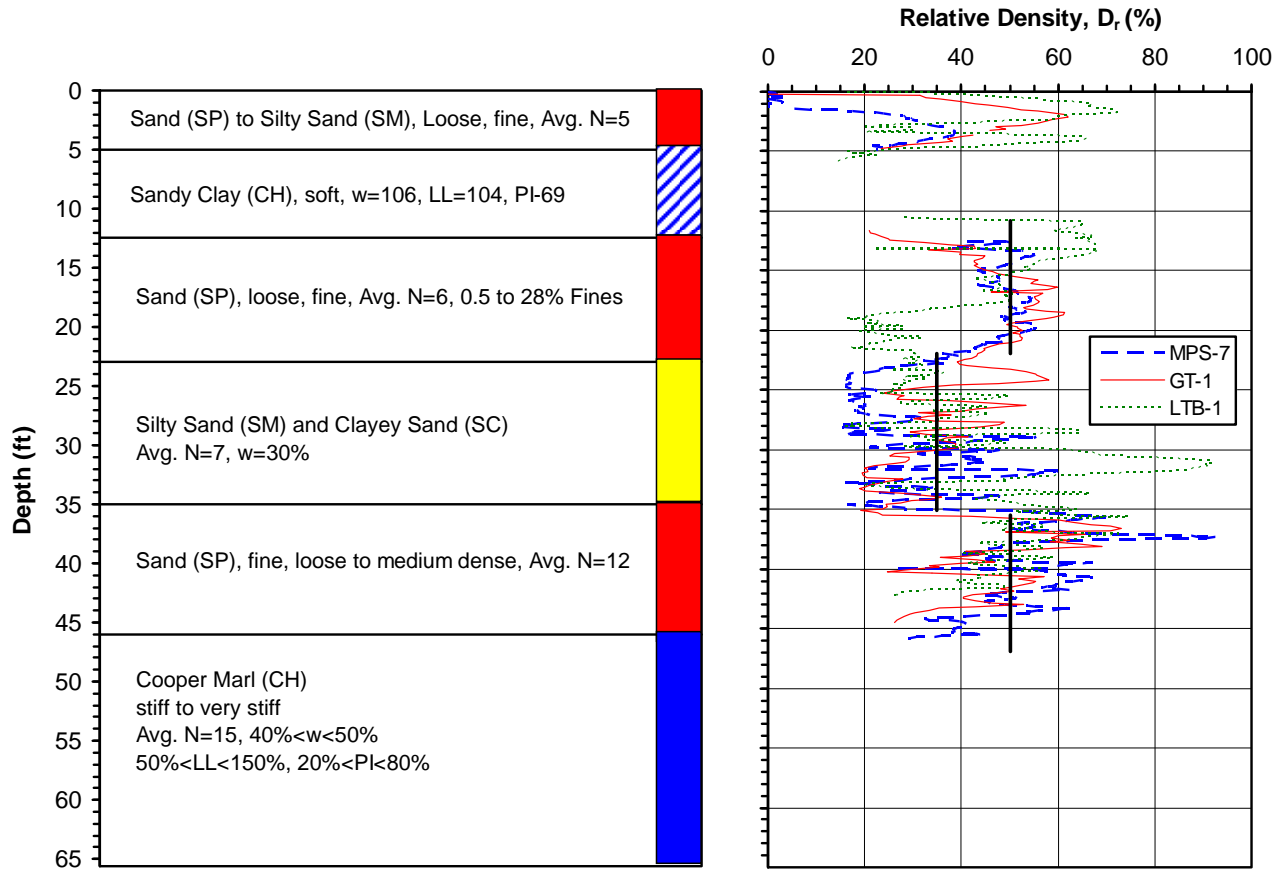


Figure 1. Idealized soil profile for the test site (Camp et al., 2002).

between 18 and 28 ft (5.5 and 8.5 m) below the ground surface. This layer contained significantly more fines and typically classified as silty sand (SM) or clayey sand (SC). The natural moisture content was 30% and the fines content varied from 15 to 24%. The fifth layer generally began at a depth of 29 ft (8.8 m) depth and extended to the top of the Marl. This layer contained fewer fines and generally classified as a loose to medium dense, poorly graded fine sand (SP).

The Cooper Marl was encountered between 42 and 46 ft (13 to 14 m) below the ground surface and extended to a depth of 280 ft (85 m), which was below the base of all the test foundations at the site. The Cooper Marl is a stiff, high plasticity calcareous silt or clay and generally classifies as MH or CH material (Camp et al 2002) according to the Unified Soil Classification System. The liquid limit typically ranges between 50 and 90% with a plasticity index varying from 15 to 60%. The natural moisture content is typically between 40 and 60% which is somewhat higher than the plastic limit but much lower than the liquid limit indicating overconsolidation. The marl is very stiff with undrained strengths typically ranging from 2000 to 4000 psf at the top of the layer and increasing with depth to a value between 4000 and 6000 psf at a depth of about 150 ft (46 m). Below this depth, the strength appears to remain relatively constant.

Cone penetration (CPT) soundings were performed at several locations near the test area. The normalized cone tip resistance (q_{c1}) for three of these soundings was used to estimate the relative density (D_r) of the coarse-grained layers using an equation developed by Kulhawy and Mayne (1990) for clean young normally consolidated sands. The relative density profiles computed using this equation are also plotted in Figure 1. In two of the sand layers the average relative density is approximately 50%; while, in the silty sand layer the relative density drops to about 35%.

FOUNDATION CHARACTERISTICS AND TEST LAYOUT

Test Foundations

The test shafts for the actuator test (MP-1) and the statnamic test (MP-3) were 8.5 ft (2.59 m) outside diameter, cast-in-steel-shell (CISS) piles. The steel casing, with a thickness of one inch, was advanced through the sand layers and into the Cooper Marl at a depth of 53 ft using a vibratory hammer. The casing was then drilled out and the hole was advanced through the Marl to a depth of 154 ft without casing. The hole was then filled with concrete using a tremie pipe. Based on 10 tests, the concrete had an average 30-day compressive strength of 5.4 ksi. The vertical reinforcement consisted of 36 #18 bars evenly distributed around a circle with a diameter of 7 ft. Confinement for the vertical steel was provided by #6 bar spirals with a pitch of 3.5 inches. A three inch concrete cover was maintained between the spiral reinforcement and the inside of the steel case.

Load Test Layout and Instrumentation

For the hydraulic actuator tests, the load was applied at a height of 1.74 ft above the ground surface using two MTS actuators acting in parallel, each capable of producing 600 kips of force. To provide a reaction, another pile with nearly identical properties was constructed approximately 28 ft from test pile MP-1 on centers. The actuators were connected to each pile with a pinned connection to provide a free-head condition. This connection allowed the application of cyclic compressive and tensile forces. Each actuator was controlled with an electromechanical servo-valve and an electric hydraulic pump. Two LVDTs were set up to measure displacements of the pile head. They were mounted to a reference beam supported by driven piles within isolation casings. The LVDTs were attached to MP-1 at heights of 1.74 ft and 4.38 ft above the ground surface. Therefore, the lower LVDT was in line with the point load application on MP-1. Four load cells on each of the two actuators provided a direct measurement of the applied load. Additional details regarding the hydraulic actuator tests are provided by Rollins et al (2005b).

For the statnamic load tests the load was applied at height of 4.3 ft above the ground surface on shaft MP-3 as shown in Figure 2. The statnamic load sled weighed approximately 70 tons and was supported on a “runway” composed of steel H sections which were in turn supported by driven piles. Applied load was measured by a load cell on the piston section of the statnamic device and pile head deflection was measured using LVDTs. In addition, two accelerometers were attached to the pile head so that deflection could be determined by double integration. In addition, a string of downhole accelerometers was installed to make measurements at eight depths within an inclinometer cast into the test shaft

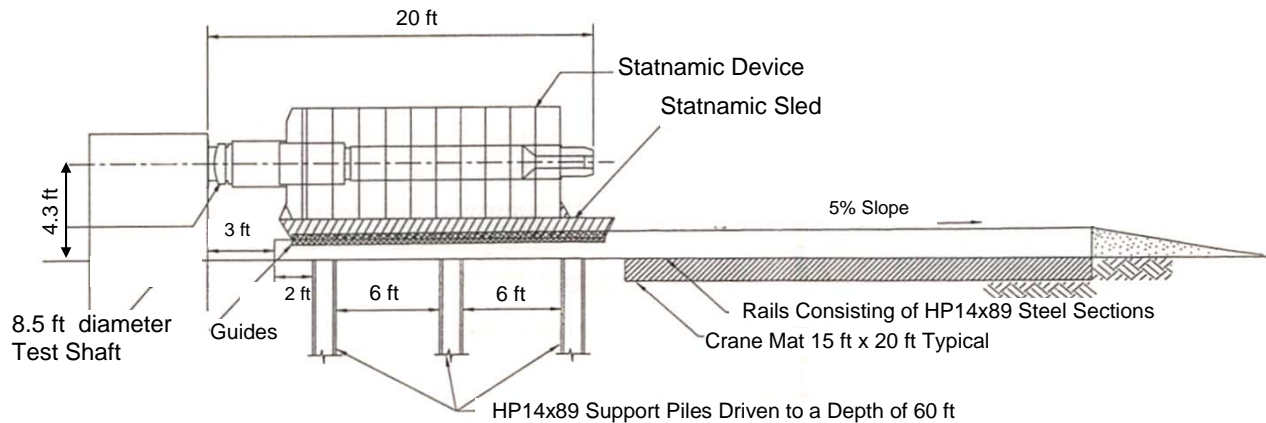


Figure 2. Test setup for lateral statnamic load tests.

Prior to concrete placement, resistance-type strain gauges were mounted on “sister bars” composed of a 3 ft long #4 bars and tied into the rebar cage at 10 depth intervals. At each strain gauge station, two strain gauges were mounted on opposite sides of the pile separated by a distance of about 7 ft. The gauges were oriented to be in line with the direction of loading. All of the pile data (load, deflection, acceleration and strain) was monitored via a data acquisition system.

To quantify the build-up and dissipation of pore pressure after blasting, piezometers were installed at various distances and depths around the test piles. The location and depth of each piezometer for the statnamic testing are shown in Figure 3, but the layout was similar for the static test. Basically, three vertical arrays were installed at radii of 6, 24, and 34 ft from the center of the test shaft. All the piezometers were distributed around the front of the pile in the direction of loading to track the variation in pore water pressure with applied load. Transducers identified with a “B” employed piezoresistive transducers identical to those at Treasure Island (Ashford et al, 2004) while those identified with an “A” used electrical resistance transducers (Rollins et al 2005c). The electrical resistance transducers were more sensitive to damage during blasting and several transducers closest to the explosive charges were damaged during blasting while those further from the charges provided some useful information. Additional information regarding pore pressure transducer selection, installation, and performance is provided by Rollins et al (2005c).

Liquefaction is manifest by an increase in pore water pressure. This increase in pore water pressure was achieved by detonating explosive charges distributed around the test shafts. A pilot liquefaction test was performed at a location separate from the foundation test sites to better define the charge weight, spacing, and delay sequence necessary to produce liquefaction. For each of the three statnamic load tests, eight charges spaced evenly around three different radii were detonated. The first eight blast holes were spaced around a radius of 13 ft. The second and third blast rings radii were 15 and 17 ft, respectively as shown in Figure 3. The charges were staggered to help avoid sympathetic detonations. The first blast series used a 1.5 lb charge at 10, 20, 30, and 38.5 ft below the ground surface. The second blast series used 2 lb charges at 15, 25, and 35 ft depths. The third and final blast series put 1.5 lb charges at the same depths as in the first blast series. The charges and layout for the actuator test were similar. The binary explosives

consisted of a mixture of ammonium nitrate and nitro-methane, and the weights are given in equivalent weights of TNT. During each of the three blast sequences, the charges were detonated two at a time with a delay of 250 milliseconds between detonations. The charges were detonated beginning around the bottom ring and then moved upward around each subsequent ring to the top.

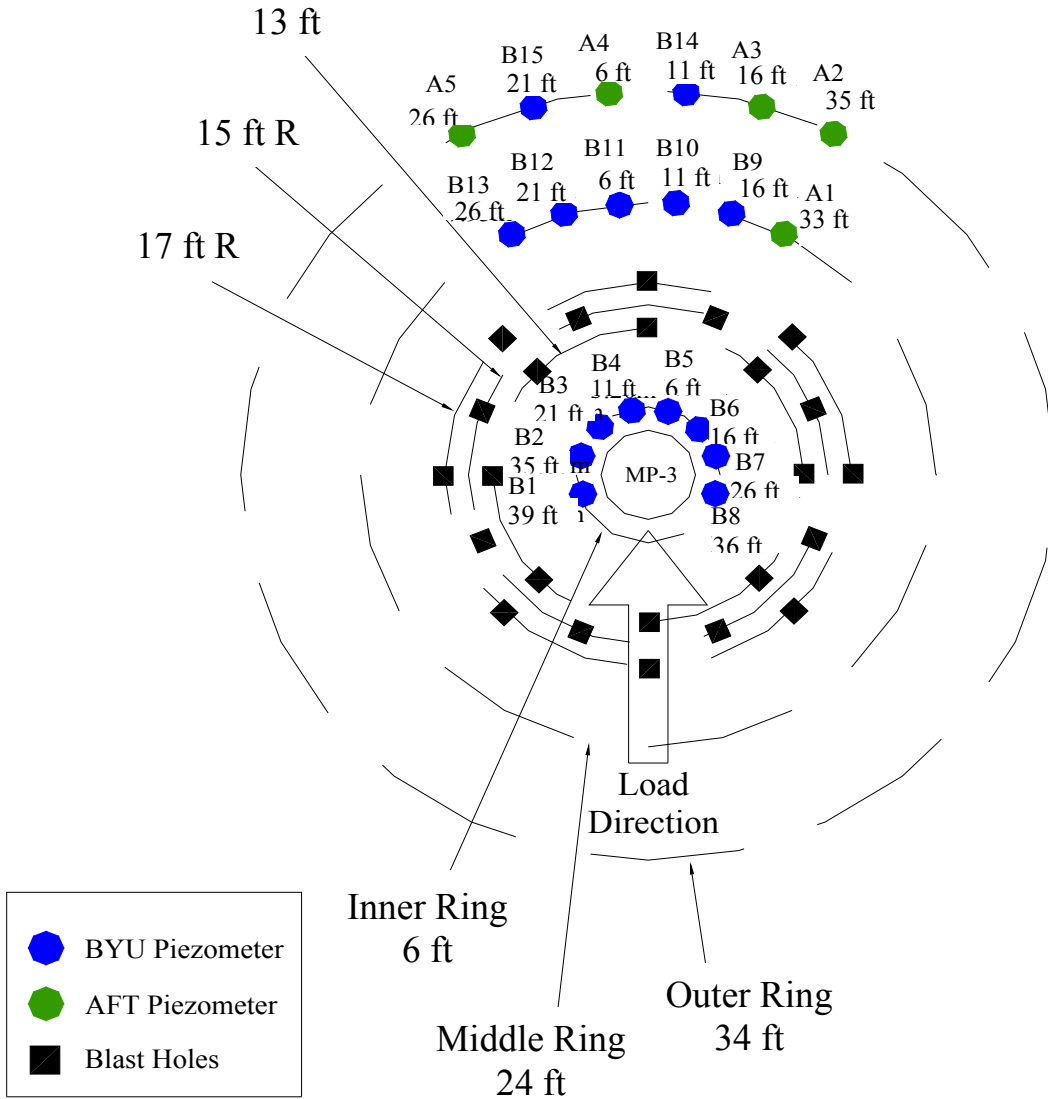


Figure 3. Plan view with layout of last holes and piezometers relative to test shaft.

STATIC LATERAL LOAD TESTS RESULTS

Prior to the lateral load testing, the explosive charges were detonated as described previously. The excess pore water pressures developed by the charges were measured by each piezometer and used to compute the excess pore pressure ratio, R_u with the equation

$$R_u = \frac{u_f - u_i}{\sigma'_o} \quad (1)$$

where u_f is the piezometer reading of pore water pressure during testing, u_i is the measured pore water pressure prior to blasting, and σ'_o is the initial vertical effective stress in the soil prior to blasting. The vertical effective stress was calculated using a moist unit weight above the water table of 113 lbs/ft³ and a saturated unit weight of 127.1 lbs/ft³ below the water table, which was at a depth of 1.52 m during testing. As can be seen in Eq. 1, when the excess pore water pressure increases and equals the effective stress, $R_u = 1.0$ or 100% and the soil is fully liquefied. A plot of the peak residual excess pore pressure ratio versus depth for each ring of piezometers is provided in Figure 4(a). The R_u values are typically between 75 and 100% throughout most of the sandy soil layers. R_u values are somewhat lower in the sand clay layer at a depth from 5 to 10 ft and at the bottom of the profile.

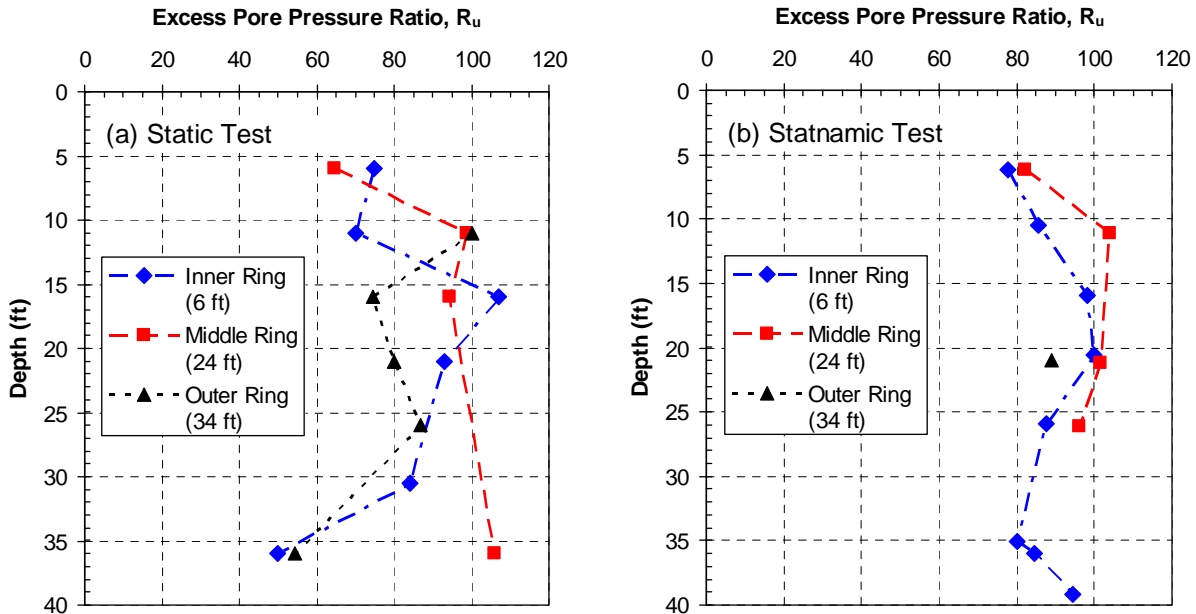


Figure 4. Peak excess pore pressure ratio versus depth profiles from three rings of piezometers during the (a) first static test and (b) the first statnamic test.

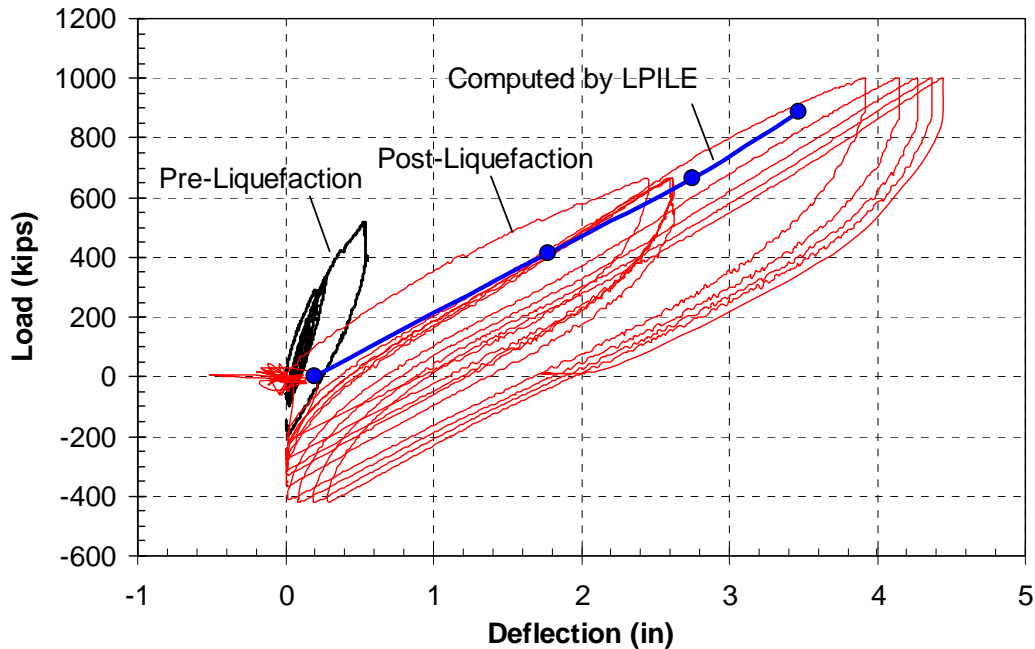


Figure 5. Measured lateral load-deflection curves for static load test before and after blast liquefaction along with curve computed by LPILE with back-calculated p-y curves.

The load vs. deflection curves before and after the detonation of the explosive charges are presented in Figure 5. As was observed in the TILT project, there is a significant decrease in stiffness after the build up of high excess pore pressure ratios (Rollins et al., 2005a). Approximately 6 to 7 times more movement is required to develop the same lateral resistance as that prior to blasting. This decrease in lateral resistance is somewhat less than that observed in the TILT experiments and may result from the fact that the percentage of lateral resistance carried by the large diameter shaft itself is much larger than that for the smaller diameter piles used in the TILT project. Because sand flowed into the space behind the pile during loading, it became necessary to apply a tensile force (negative sign) to pull the pile back to the initial position.

Both the maximum moment and the depth to the maximum moment increased substantially following blasting because of the reduced soil resistance due to pore pressure development in the loose sand. After the blast, the maximum moment for a given load increased by about 100% in comparison with the pre-blast value. Prior to blasting, the maximum moment occurred at a depth of about 20 ft; however, after liquefaction, the maximum moment occurred near the interface with the Marl at a depth of 42 ft.

Rollins et al (2005b) used the bending moment and displacement data to back-calculate p-y curves for the liquefied sand and clay at the test site. These curves were in good agreement with p-y curves predicted using the equation

$$p = A (By)^C p_d \quad (2)$$

developed by Rollins et al (2005a) for the TILT project. In this equation, the lateral soil pressure per length of pile (p) in kN/m in liquefied sand is expressed as a function of horizontal pile deflection (y) in mm. Eq. 2 was developed for sands with D_r of about 50%, while sands with a D_r

of about 35% were found to produce no resistance. In Eq. 2, $A = 3 \times 10^{-7}(z+1)^{6.05}$, $B = 2.80(z+1)^{0.11}$, $C = 2.85(z+1)^{-0.41}$, $z =$ depth in meters, and $p_d = 3.81 \ln d + 5.6$ where d is the pile diameter in meters. The p_d value was 9.2 for the 8.5 ft diameter pile. The back-calculated p - y curves were then used along with the non-linear pile properties to conduct a lateral load analysis with the computer program LPILE plus version 5.0.12 (Reese et al, 2004). The computed load-deflection curve is presented in Figure 5 and the agreement with measured response is very good.

STATNAMIC LATERAL LOAD TEST RESULTS

Prior to each statnamic lateral load test, the explosive charges were detonated as described previously. After a period of about 30 seconds to allow gases from the blast holes to vent, the fuel pellets in the statnamic load sled were ignited. A plot of the peak residual excess pore pressure ratio vs. depth for each ring of piezometers is provided in Fig 4(b). The residual R_u values were typically between 80 and 100%. Once again, the R_u values at 6 to 10 ft below the ground surface were lower than 100% because of the high clay content in this layer.

The dynamic load versus deflection curve for the second statnamic load test is shown in Figure 6. The rise time for the applied statnamic load was approximately 0.1 second, while the total duration of loading was about 0.27 seconds. As the load level increased for a given test, the rise time decreased. As shown in Figure 6, the peak deflection occurred some time after the peak load. In fact, the applied load is only about 10% of the maximum load when the peak deflection occurs. The shape of the loop suggests that damping is playing a significant role in the lateral pile resistance.

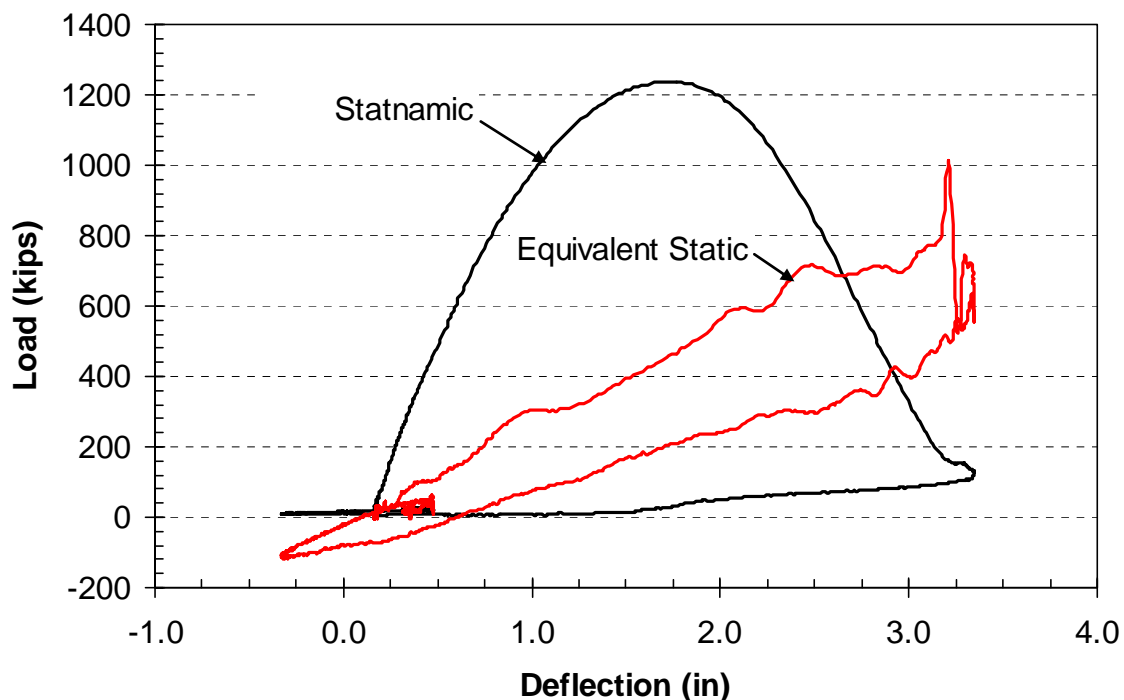


Figure 6. Dynamic load versus deflection curve for second statnamic load test along with interpreted equivalent static load versus deflection curve.

ANALYSIS OF STATNOMIC TEST RESULTS

The load measured by the statnomic load cell (F_{stn}) includes the contribution to load provided by inertia, damping, and static soil resistance. The large loop in the load versus deflection curve indicates that damping is a significant component of the total load. The static soil resistance (F_s) can be computed by subtracting the inertial and the damping forces for a lumped mass model from the measured statnomic force using the equation

$$F_s = F_{\text{stn}} - \Sigma M_i a_i - \Sigma C_i v_i \quad (3)$$

where M_i is the mass of a given segment of the shaft, a_i is the acceleration of the segment, C_i is the damping coefficient for the segment, and v_i is the velocity of the segment. Because the acceleration was measured at 8 depth intervals along the shaft as well as at the top of the shaft, the inertia force could be readily determined as a function of time during each statnomic test. In addition, the acceleration time histories at each depth could be integrated to obtain velocity time histories for each segment of the shaft. The most significant difficulty lies in estimating an appropriate damping coefficient. For this study, this value was estimated based on the log-decrement method. Although conditions after the statnomic loading do not strictly correspond to “free-vibration” conditions, it is close enough that an estimate of the damping ratio can be obtained. Based on this approach the damping ratio for the three statnomic load tests was found to be between 0.30 and 0.35. Using Eq. 3, the interpreted static lateral resistance versus deflection curve for the second statnomic test was determined and it is plotted in Figure 7. In comparison with the dynamic load versus deflection curve, the static curve is far more linear, as expected.

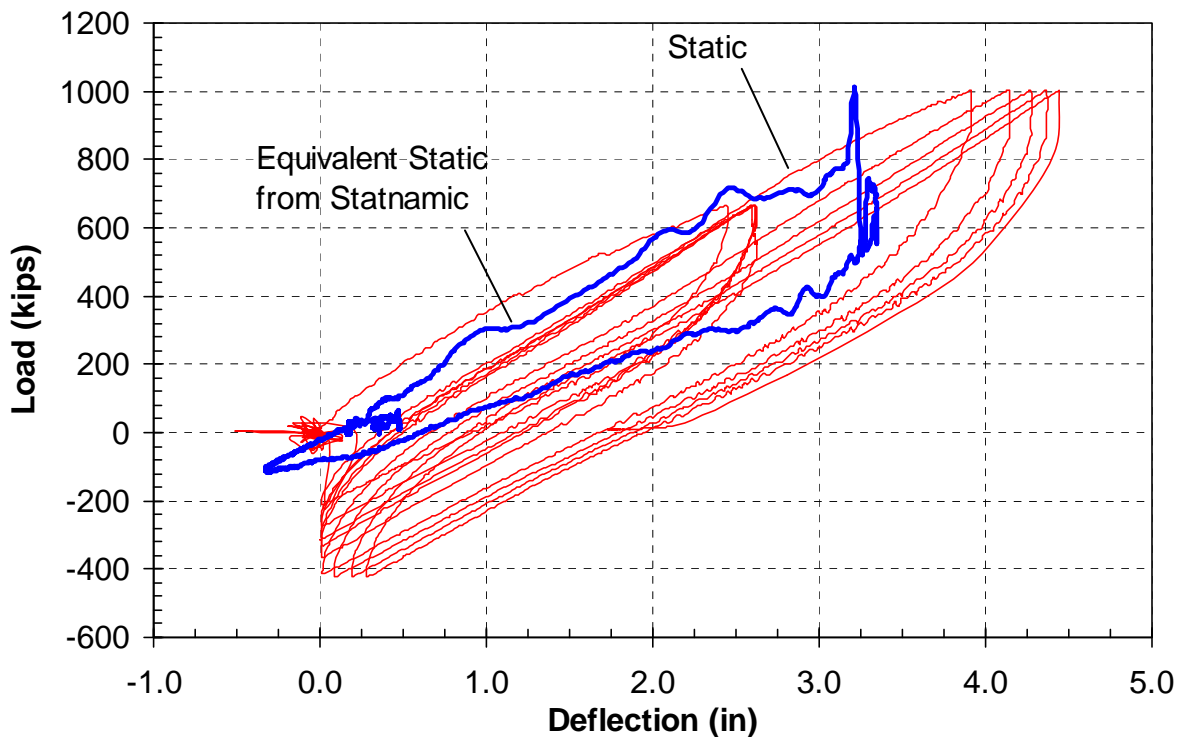


Figure 7. Comparison of equivalent static load-deflection curve interpreted from the statnomic tests in comparison with curve from static test with hydraulic actuators.

Although the contribution to load provided by damping is substantial, the analyses indicate that the contribution provided by inertia was much greater. Additional discussion of the dynamic analysis is provided by Rollins et al. (2007). In Figure 7 the interpreted static load vs. deflection curve from a statnamic test is compared with the static load versus deflection curve obtained from the lateral load tests performed using hydraulic actuators on test shaft MP-1. Although the curves are offset due to a difference in the initial starting point for the static load test, the slope of both curves is remarkably similar. In addition, the shape of the load-unload loop for both curves is also similar. These similarities suggest that the damping ratio used to interpret the static load-deflection curve from the statnamic test is reasonable.

To evaluate the applicability of Eq. 3 for the statnamic load tests, lateral pile load analyses were again carried out using the computer program LPILE (Reese et al, 2004). The p-y curve shapes, layer thicknesses and soil properties used in the analyses are summarized in Table I. Within the liquefied zone, two cases were investigated. For the first case, the resistance in the entire liquefied zone (11.5 to 41 ft) was considered to be zero, which is a worst case situation. For the second case, the resistance in the liquefied zone was assumed to be zero when the D_r was 35%, but was defined by Eq. 3 when D_r was about 50%. The load versus deflection curve computed for the first case assuming no resistance in the liquefied zone is much softer than the measured curve obtained from field testing. However, the curve computed for the second case where the p-y curves in the liquefied sand were based on Eq. 3 with a p_d value of 9.2, the computed load-deflection curve agrees favorably with the measured curve.

TABLE I. SOIL PROPERTIES USED IN THE LATERAL PILE LOAD ANALYSIS WITH LPILE.

Depth interval	p-y Curve Shape	γ' (lbs/ft ³)	ϕ (°)	K (lb/in ³)	C (lbs/ft ²)	ϵ_{50}
0-5 ft	API Sand (API, 1983)	124.2	38	216	0	-
5-11.5 ft	Soft Clay (Matlock, 1970)	63.7	0	-	Linear 500-1000	0.02
11.5 -23 ft	Liquefied Sand ($D_r=50\%$) (Rollins et al, 2005)	60.5	Resistance from Eq. 3			
23-34.5 ft	Liquefied Sand ($D_r=35\%$) (Rollins et al, 2005)	60.5	No Resistance			
34.5-41 ft	Liquefied Sand ($D_r=50\%$) (Rollins et al, 2005)	60.5	Resistance from Eq. 3			
41-104 ft	Cooper Marl (Reese et al, 1975)	64.6	0	500	4140	0.005

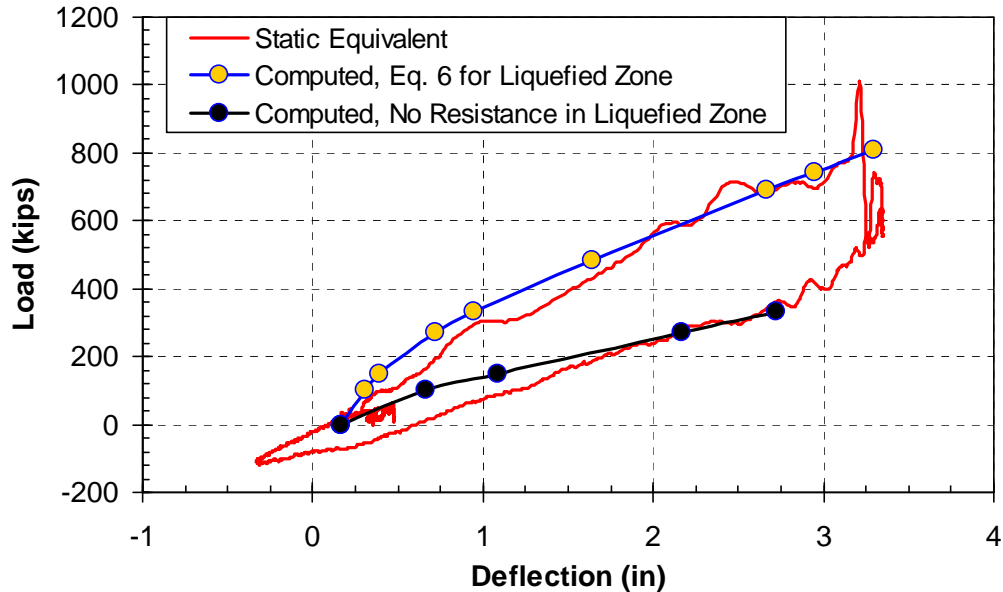


Figure 8. Comparison of interpreted static load versus deflection curve from statnamic test with curves predicted by LPILE assuming (a) no soil resistance in liquefied zone and (b) p-y curves for liquefied sand in $D_r=50\%$ sand proposed by Rollins et al (2005a).

CONCLUSIONS

1. The blast liquefaction technique in combination with the statnamic lateral load procedure provides a viable means for evaluating the dynamic lateral resistance of deep foundations in liquefied sand under full-scale conditions. These tests can be particularly valuable in evaluating foundation behaviour for important structures.
2. The increased resistance provided by the 8.5 ft diameter test pile could be reasonably approximated using the equations proposed by Rollins et al. (2005a) for a 12 in diameter pile with a diameter correction factor (p_d) of about 9.
3. The interpreted static lateral resistance from the statnamic test using a lumped mass approach was approximately the same as the static lateral resistance measured in hydraulic actuator tests on an adjacent test shaft at the same site.
4. The damping ratio for the 8.5 ft diameter drilled shaft in liquefied sand during the statnamic testing was approximately 30 to 35%.
5. The interpreted static load-deflection curve indicates that the liquefied sand provided significant lateral resistance and that a reasonable estimate of the response could be obtained using p-y curves for liquefied sand ($D_r \approx 50\%$) developed by Rollins et al (2005a) which include diameter effects.

ACKNOWLEDGEMENTS

Funding for the full-scale load tests was provided by the South Carolina Department of Transportation and Modern Continental South was the contractor for the testing program.

Applied Foundation Testing installed the strain gages, piezometers, and LVDTs and was responsible for data acquisition. Financial support for the analysis of the test results was provided by the National Science Foundation under Grant No. CMS-0085353. This funding is gratefully acknowledged. Nevertheless, the opinions and conclusions in this paper do not necessarily reflect the views of the sponsors.

REFERENCES

- American Petroleum Institute [API]. (1993). Recommended Practice for Planning, Designing, and Constructing Fixed Offshore Platforms. API RPA-WSD, 20th Edition.
- Ashford, S.A., Rollins, K.M., and Lane, J.D. (2004). "Blast-induced liquefaction for full-scale foundation testing." *J. Geotechnical and Geoenv. Engrg.*, ASCE, Vol. 130 (8), p. 798-806.
- Camp, W.M., Brown, D.A., and Mayne, P.W. (2002). "Construction method effects on axial drilled shaft performance." *Deep Foundations 2002, GTP No. 116*, ASCE, Vol. 1, p. 193-208.
- Kulhawy, F. H., and Mayne, P. W. (1990). Manual on estimating soil properties for foundation design. Research Project 1493-6, EL-6800, Electric Power Research Institute. Palo Alto, California.
- Matlock, H. (1970). "Correlations for design of laterally-loaded piles in soft clay" *Procs., Second Annual Offshore Technology Conf.*, Paper No. OTC 1204, Vol. 1, p. 577-594.
- Reese, L.C., Cox, W.R., and Koop, F.D. (1975). "Field testing and analysis of laterally loaded piles in stiff clay." *Proceedings*, Offshore Technology conference, Houston, Texas, Paper No. 2312, p. 671-690.
- Reese, L.C., Wang, S.T., Isenhower, W.M. and Arrellaga, J.A. (2000). "Computer program LPILE plus version 5.0 users manual," Ensoft, Inc., Austin, Texas.
- Rollins, K.M., Gerber, T.M., Lane, J.D. and Ashford, S.A. (2005a). "Lateral resistance of a full-scale pile group in liquefied sand." *J. Geotechnical and Geoenv. Engrg.*, ASCE, Vol. 131 (1), p. 115-125.
- Rollins, K.M., Hales, L.J., Ashford, S.A. and Camp, W.M. III (2005b). "P-Y curves for large diameter shafts in liquefied sand from blast liquefaction tests." *Geotechnical Special Publication No. 145*, Ed. Boulanger, R.W. and Tokimatsu, K., ASCE, p. 11-23.
- Rollins, K.M., Lane, J.D., Dibb, E., Ashford, S.A., Mullins, A.G. (2005c). "Pore pressure measurement in blast-induced liquefaction experiments." *Transportation Research Record 1936*, "Soil Mechanics 2005," TRB, Washington DC, p. 210-220.
- Rollins, K., Bowles, S., Brown, D., Ashford, S. (2007). "Lateral load testing of large drilled shafts after blast-induced liquefaction." *Procs. 4th Intl. Conf. on Earthquake Geotechnical Engrg.*, Springer, Paper 1141 (CD-Rom).
- Suzuki, H. and Tokimatsu, K. (2003). "Effect of pore water pressure response around pile on p-y relation during liquefaction." *Procs. 11th Intl. Conf. on Soil Dynamics and Earthquake Engineering*, Stallion Press, Vol. 2, p. 567-572.
- Weaver, T.J., Ashford, S.A. and Rollins, K.M. (2005). "Lateral resistance of a 0.6 m drilled shaft in liquefied sand." *J. Geotechnical and Geoenv. Engrg.*, ASCE Vol. 131 (1), p. 94-102.
- Wilson D.W., Boulanger, R.W. and Kutter, B.L (2000). "Observed seismic lateral resistance of liquefying sand." *J. Geotechnical and Geoenv. Engrg.*, Vol. 126 (10), p. 898-906.